IBRO Neuroscience Reports 14 (2023) 494–506

Contents lists available at ScienceDirect

IBRO Neuroscience Reports

journal homepage: www.sciencedirect.com/journal/IBRO-Neuroscience-Reports

Research paper

Olfactory bulbectomy induces nociceptive alterations associated with gliosis in male rats

Gumaro Galindo-Paredes [a,b], Gonzalo Flores [c], Julio César Morales-Medina [a,*]

[a] Centro de Investigación en Reproducción Animal, CINVESTAV-Universidad Autónoma de Tlaxcala, AP 62, CP 90000 Tlaxcala, Mexico
[b] Departamento de Fisiología, Biofísica y Neurociencias, Centro de Investigación y de Estudios Avanzados del Instituto Politécnico Nacional, Cinvestav del IPN, Av. IPN 2508, San Pedro Zacatenco, 07360 Ciudad de México, Mexico
[c] Lab. Neuropsiquiatría, Instituto de Fisiología, Benemérita Universidad Autónoma de Puebla, 14 Sur 6301, San Manuel 72570, Puebla, Mexico

ARTICLE INFO

Keywords:
Allodynia
Bulbectomy
Depression
Nociception
OBX

ABSTRACT

Major depressive disorder (MDD) is a major health concern worldwide with a wide array of symptoms. Emerging evidence suggests a high comorbidity between MDD and chronic pain, however, the relationship between these two diseases is not completely understood. Growing evidence suggests that glial cells play a key role in both disorders. Hence, we examined the effect of olfactory bulbectomy (OBX), a well-known model of depression-related behavior, on nociceptive behaviors and the number and morphology of astrocytes and glial cells in brain regions involved in the control of nociceptive processes in male rats. The brain regions analyzed included the basolateral amygdala (BLA), central amygdala (CeA), prefrontal cortex (PFC), and CA1 subregion of the hippocampus. A battery of behavioral tests, mechanical allodynia, thermal cold allodynia and mechanical hyperalgesia, was evaluated before and four weeks after OBX. Quantitative morphological analysis, as well as assessment of the number of glial fibrillary acidic protein (GFAP) and ionizing calcium-binding adaptor molecule 1 (Iba1) positive astrocytes and microglia were carried out to characterize glial remodeling and density, respectively. OBX caused mechanical and cold allodynia in an asynchronous pattern. The cold allodynia was noticeable one week following surgery, while mechanical allodynia became apparent two weeks after surgery. In the BLA, CeA and CA1, OBX caused significant changes in glial cells, such as hypertrophy and hypotrophy in GFAP-positive astrocytes and Iba1-positive microglia, respectively. Iba1-positive microglia in the PFC underwent selective hypotrophy due to OBX and OBX enhanced both GFAP-positive astrocytes and Iba1-positive microglia in the BLA. In addition, OBX increased the number of GFAP-positive astrocytes in the CeA and CA1. The amount of Iba1-positive microglia in the PFC also increased as a result of OBX. Furthermore, we found that there was a strong link between the observed behaviors and glial activation in OBX rats. Overall, our work supports the neuroinflammatory hypothesis of MDD and the comorbidity between pain and depression by demonstrating nociceptive impairment and significant microglial and astrocytic activation in the brain.

1. Introduction

Major depressive disorder (MDD) is a mood disorder with multiple symptomology including anhedonia, guilt, low self-esteem, loss of interest, memory problems, pain and sadness (Yanguas-Casas et al., 2020; Dolotov et al., 2022; Zhao et al., 2022). Depression is the most common mental disorder, affecting more than 300 million people worldwide with a prevalence of 4.4% (WHO, 2017; Hanson et al., 2022). Interestingly, the prevalence of chronic pain is over 50% in patients with MDD (von Knorring et al., 1983). In addition, chronic pain patients have a comorbidity MDD reported between 20% and 85% (Carroll et al., 2004). Furthermore, pain could affect MDD prognosis and treatment and vice versa (Doan et al., 2015). Finally, Fishbain et al. (1997) suggested a correlation between MDD and pain severity. All these data point to an association between pain and MDD.

There are several recognized mechanisms involved in MDD, including the neuroimmune hypothesis of depression (Jesulola et al., 2018). This hypothesis suggests that glia are the causal agent of this disorder (Miller & Raison, 2016; Wohleb et al., 2016). Glia constitute the greater number of cells within the central nervous system (CNS) and are comprised of microglia, astrocytes, ependymal cells and oligodendrocytes (Jesulola et al., 2018). In support of the neuroimmune hypothesis,

* Correspondence to: Centro de Investigación en Reproducción Animal, Km 10.5 carretera San Martin Texmelucan, Ixtacuixtla, Tlaxcala 90128, Mexico.
E-mail address: jmoralesm@cinvestav.mx (J.C. Morales-Medina).

https://doi.org/10.1016/j.ibneur.2023.05.006
Received 15 January 2023; Received in revised form 12 May 2023; Accepted 13 May 2023
Available online 17 May 2023

postmortem studies of suicide patients with MDD showed a reduction in glial density in the medial prefrontal cortex (PFC) (Ongur et al., 1998; Cotter et al., 2001; Si et al., 2004) and astrocytic hypertrophy in the anterior cingulate cortex (ACC) (Torres-Platas et al., 2011). In contrast, glial density was increased in the pyramidal and granule cell layers of the hippocampus (Stockmeier et al., 2004). Data from animal models of stress or depression-related behavior have shown contrasting patterns of astrocyte and microglial characteristics in the CNS (Sanacora & Banasr, 2013; Naskar & Chattarji, 2019; Codeluppi et al., 2021), therefore; further analysis is required to understand the contribution of glia to MDD.

Olfactory bulbectomy (OBX) is a well-known, validated rat model of depression that results in behavioral and neurochemical deficits similar to the human condition (Kelly et al., 1997; Morales-Medina et al., 2017). In the open field test (OFT), OBX rats display hyperlocomotion, which was interpreted as a failure of adaptation to novelty (Kelly et al., 1997; Morales-Medina et al., 2012a; Almeida et al., 2017; Morales-Medina et al., 2017). While this behavior has been well-established and reproduced across research groups, nociceptive tasks have been given little attention. Burke et al. (2013) observed that OBX induced mechanical allodynia two weeks after surgery. Moreover, three weeks after OBX, Burke et al. (2013) observed increased mRNA expression in the amygdala of glial fibrillary acidic protein (GFAP) and cluster of differentiation molecule 11b (CD11b), putative markers of astrocytes and glia. It remains to be investigated whether protein levels, as well as the density or morphology of astrocytes and microglia, are modified. This study seeks to evaluate whether OBX modifies the density and structure of astrocytes and microglia in brain regions involved in nociception such as the hippocampus (HPO), the PFC, the basolateral (BLA) and central amygdala (CeA). Therefore, this study attempts to further elucidate the relationship between depression, pain, and neuroinflammation.

2. Material and methods

2.1. Study design

One cohort of rats was used for our present experiments to test the behavioural and glial consequences of OBX (Fig. 1).

2.2. Animals and housing

At the Centro de Investigacion en Reproduccion Animal (CINVESTAV, Mexico), male (n = 19) Wistar rats (*Rattus norvegicus*) were housed three to four per cage in a room maintained on a 12-hour light/dark cycle with standard temperature (20 °C) and humidity (30%). Rats had ad libitum access to food and water. Rats were about two months old at the beginning of the study. All procedures complied with the National Institutes of Health Guide, the technical guidelines for animals in the laboratory issued by SAGARPA Mexico (NOM-062 ZOO-1999) and ARRIVE guidelines (Kilkenny et al., 2010). During experimentation, any animals showing signs of distress were assessed by a veterinarian and, if necessary, euthanized to minimize animal suffering.

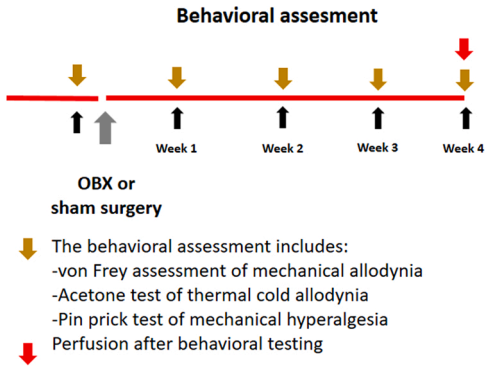

Fig. 1. Schematic for experimental design. *Abbreviation: Olfactory bulbectomy, OBX.*

2.3. OBX surgery

OBX was achieved as previously described (Morales-Medina et al., 2012b; Morales-Medina et al., 2013b). In summary, rats received a ketamine/xylazine cocktail (0.75 ml ketamine/0.35 ml xylazine/5 ml sterile saline, injected 0.25 ml per 20 g, i.p). to induce anesthesia. Once rats were fully anesthetized, a cranial window was created in the frontal bone, 5.2 mm anterior to bregma. The olfactory bulbs were cut and aspirated out for the OBX procedure, while sham operations received identical surgery, except the bulbs were left intact. The prevention of blood loss from the cranial window was achieved by filling the open space with a hemostatic sponge (Gelfoam, Pfizer Inc., Kalamazoo, MI). After surgery, rats were administered a saline solution (0.9% NaCl) and returned to their cages to recover for four weeks. Following brain harvest, only those brains in which the olfactory bulbs were completely removed without damaging the PFC were included in data analysis.

2.4. Behavioral testing

The study evaluates three nociceptive assays in male rats.

2.4.1. von Frey assessment of mechanical allodynia

In brief, two days prior to OBX surgery, rats underwent a baseline (BL) mechanical threshold test (Bautista-Carro et al., 2021; Cooper et al., 2022). First, rats were acclimated to individual Plexiglas boxes (20 ×13 x 10 cm) on a stainless steel grid for 60 min. Second, rats were tested for BL mechanical thresholds using von Frey filaments (Stoelting Inc., IL, USA). The mid-plantar region of the hind paw was stimulated with an incremental series of eight monofilaments of logarithmic stiffness to determine the 50% withdrawal threshold (Chaplan et al., 1994). Here, an intermediate filament (number 4.31 exerting 2.0 g of force) was applied perpendicular to the skin, causing a slight bending. In case of a positive response (rapid withdrawal or licking of the paw within 3 s), the next smaller filament was tested. In case of a negative response, the next larger filament was tested. Testing continued until four measurements beyond the first change were taken. After OBX surgery, mechanical responses and paw thickness were evaluated as described for BL mechanical threshold testing once weekly for four weeks.

2.4.2. Acetone test of thermal cold allodynia

Once mechanical thresholds were measured, acetone testing was performed in the same boxes. A drop of acetone was applied to the plantar surface of the paw using a 1 ml syringe (Moriarty et al., 2012). Approximately, 0.2 ml of acetone was administered to the plantar surface of the hindpaw avoiding mechanical stimulation. Each hindpaw was tested 2 times, alternating between left and right paws. The number of positive responses was measured for one minute. Shivering, licking or removing the paw were regarded as a positive response. The interval between tests was at least 3 min

2.4.3. Pin prick test of mechanical hyperalgesia

Next, we applied the sharp edge of a dull pin to both hindpaws without damaging the skin (Taylor et al., 2007). The withdrawal latency was monitored for one minute. At least one min elapsed between testing of the left and right hindpaws. After all nociceptive assays, paw thickness was determined with a caliper.

2.5. Inmunohistochemistry

After behavioral testing, rats were deeply anesthetized with a ketamine/xylazine cocktail and perfused transcardially with 1X phosphate buffered saline (PBS) (pH 7.4), followed by 4% paraformaldehyde in PBS

as previously reported (Monfil et al., 2018; Morales-Medina et al., 2020). The brains were post-fixed overnight at 4 °C in paraformaldehyde. Coronal brain sections (40-μm-thick) were cut in four series with a vibratome (Vibratome 1000 Plus, Leica microsystems, Buffalo Grove, IL) and placed in 1x PBS. The sections were then transferred to a cryoprotectant solution (glycerol : ethylene glycol : PBS, 3:3:4) and stored at − 20 °C until processed for immunohistochemistry.

A standard avidin-biotin protocol was used in the present study (Gonzalez-Granillo et al., 2022). For GFAP staining, the sections were washed in 1X PBS for 5 min (3 times), incubated in 1.5% hydrogen peroxide for 5 min and washed twice in 1X PBS (5 min). The sections were then incubated in antisera diluent [PBS + 3% normal rabbit serum (NRS) + 0.3% Triton X-100] for 120 min and transferred into the primary antibody (goat anti-GFAP, ab53554–52, Abcam, CA, USA) at 1:500 dilution in antisera diluent (PBS+1% NRS+0.3% Triton X-100) and incubated overnight at 4 °C. The next day, sections were washed in 1X PBS for 5 min (3 times). Sections were processed using a Rabbit Vectastain ABC kit from Vector Laboratories (PK-4001, Burlingame, CA, USA). Subsequently, sections were incubated with diaminobenzidine for 2.5 min (DAB substrate kit, SK-4100, Vector Laboratories, Burlingame, CA, USA). Lastly, sections were mounted onto slides, air dried and coverslipped. For ionizing calcium-binding adaptor molecule 1 (Iba1) protocol, all the steps were the same except the following reagents were used: normal goat serum, anti-iba1 at 1:1000 dilution (Cell Signaling, USA) and Goat Vectastain ABC kit from Vector Laboratories (PK-4001, Burlingame, CA, USA).

For both microglial and astrocytic morphology, the following protocol was used (Morales-Medina et al., 2007; Gonzalez-Granillo et al., 2022). According to the brain atlas from Paxinos and Watson (1997), the following brain areas were examined for Iba1 and GFAP positive cells: the PFC (Fig. 9-11), BLA (fig 26–31), CeA (fig 26–31), and CA1 subfield of hippocampus (fig 27–32). The criteria used to select cells for reconstruction were previously described by our group and others (Morales-Medina et al., 2007; Morales-Medina et al., 2013a; Naskar & Chattarji, 2019). Inclusion criteria for cell reconstruction include: 1) the presence of untruncated glial processes, 2) consistent impregnation along the entire extent of all glial processes, and 3) relative isolation from neighboring cells.

An observer blind to the group identified the three-dimensional glial tree of five cells in each hemisphere (10 cells per animal per area, 5 cells per side) in 9–10 animals per group. Each cell was reconstructed with a 40X objective in a two-dimensional plane using a camera lucida (DM 2000 Microscope, Leica Microsystems, Wetzlar, Germany). Glial processes were quantified using the Sholl analysis (Sholl, 1953). A transparent grid with concentric rings, spaced 5 μm apart, was placed over the glial processes drawing, and the number of ring intersections was quantified. Moreover, the total filament length was calculated by multiplying the total number of intersections of each ring by 5 μm. The total number of glial processes (branching indicated by bifurcation) was counted at each order away from the center of the cell body to the end of the glial process.

Moreover, GFAP or Iba1 positive cells were counted manually within each neuroanatomical area at 40X magnification (Microscope Leica, model DM200, Leica microsystems, Deerfield, IL, USA). At least four sections per area were counted bilaterally and averaged using set box cages (10.9 μm^2) for each brain region.

Glial and behavior analysis was performed by a blinded observer. At the conclusion of the studies, one scientist unblinded himself from the outcomes to do data analysis.

2.6. Statistical analysis

Behavioral data were analyzed using repeated two-way ANOVA, followed by post-hoc comparisons. Additionally, the area under the curve (AUC) was considered if differences between time points were significant. Data from arborization, total filament length, and order were analyzed by two-way ANOVA, followed by post-hoc comparisons with OBX lesion, using regions and order as independent factors. For all other analyses t-test was used. Linear regression was performed between behavioral response and the number or morphology of GFAP-positive astrocytes or Iba1-positive microglial cells in OBX rats. Regions with Pearson's correlation coefficient (R) $R \geq 0.88$ were considered. Graph Pad Prism version 5.04 (California, USA) statistical software was used for all analyses and a p value less than < 0.05 was considered significant.

Data were collected and analyzed from three behavioral tests on both paws and from bilateral immunohistochemistry. Mean data for behavior tests and immunohistochemistry are expressed in the main figures, while data from individual paws or brain hemispheres, respectively, are displayed in supplemental figures.

3. Results

In the current study, mechanical thresholds and withdrawal frequencies were evaluated two days prior to OBX surgery and weekly for four weeks (Fig. 1). For GFAP and Iba1 immunohistochemistry, we evaluated the combined data as well as the left and right sides individually for all analyses.

3.1. OBX reduces mechanical thresholds in the von Frey test and increases withdrawal frequency in the acetone test in both paws

OBX significantly reduces the mechanical threshold (Fig. 2A) [Surgery $F(1,17)= 30.93$, $p \leq 0.001$; Time $F(4,68)= 7.381$, $p \leq 0.001$; Interaction $F(4,68)= 2.72$, $p \leq 0.05$] with significant differences at weeks 2, 3 and 4. The cumulative data from weeks 1 through 4 is expressed as the AUC, showing decreased mechanical thresholds (Fig. 2. B) ($p \leq 0.01$). OBX increases withdrawal frequency to an acetone drop (Fig. 2C) [Surgery $F(1,17)= 29.31$, $p \leq 0.001$; Time $F(4,68)= 5.532$, $p \leq 0.01$; Interaction $F(4, 68)= 4.29$, $p \leq 0.05$]. Of note, there were significant differences in withdrawal frequency from the first week which were maintained throughout the experiment. The cumulative acetone withdrawal frequency data from week 1 to week 4, expressed as AUC shows an increase (Fi. 2D) ($p \leq 0.01$). No modification in the withdrawal latency to a noxious stimulus (pinprick) was observed between groups (Fig. 2E). The cumulative noxious stimulus withdrawal latency data from week 1 to week 4, expressed as AUC, did not show any modification between groups (Fig. 2F). Data from left and right paws are presented in Fig. S1.

3.2. OBX increases the number and total length of filaments in GFAP-positive astrocytes and increases the number of and reduces the total filament length in Iba1-positive microglia in the BLA

Our results indicate that compared to controls (sham animals), OBX disrupts the morphology of GFAP-positive astrocytes in the BLA. The results from the total BLA indicate that OBX increases the total filament length (Fig. 3A) ($p \leq 0.001$), the arborization (Fig. 3B) [distance $F(1170)= 199.5$, $p \leq 0.001$; intersections $F(9170)= 101.4$, $p \leq 0.001$; Interaction $F(9, 170)= 10.93$, $p \leq 0.001$; distance from cell body 20–45 μm] and the number of order (Fig. 3 C) [number $F(1153)= 88.23$, $p \leq 0.001$; filament length $F(8153)= 223.5$, $p \leq 0.001$; Interaction $F(8153)= 14.86$, $p \leq 0.001$; number of order 2–4] of GFAP-positive astrocytes. OBX increases the number of GFAP-positive astrocytes in the whole BLA (Fig. 3D) ($p \leq 0.001$). Regarding microglia, OBX decreases the total filament length (Fig. 3E) ($p \leq 0.001$), the arborization (Fig. 3F) [distance $F(1170)= 166.4$, $p \leq 0.001$; intersections $F(9170)= 228.$, $p \leq 0.001$; Interaction $F(9, 170)= 5.775$, $p \leq 0.001$; distance from cell body 10–40 μm] and the number of order (Fig. 3 G) [number $F(1153)= 74.92$, $p \leq 0.001$; filament length $F(8153)= 324.1$, $p \leq 0.001$; Interaction $F(8, 153)= 8.524$, $p \leq 0.001$; number of order 2–5] of Iba1-positive microglia in the BLA. Finally, OBX increases the number of Iba1-positive

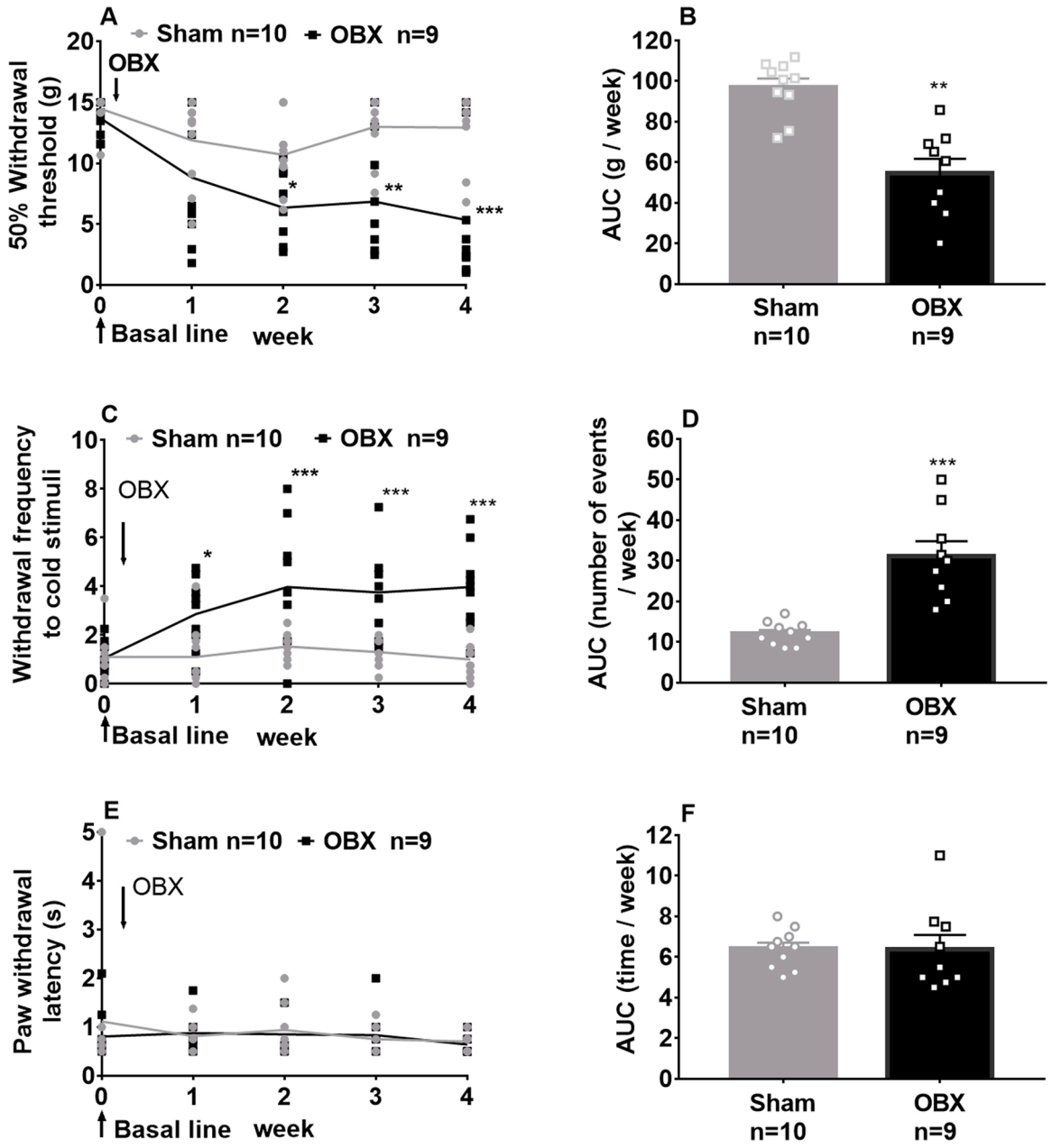

Fig. 2. OBX induces mechanical and cold allodynia in rats. Mechanical thresholds are averaged from both paws (A) at various time points before and after OBX. The AUC from data from the four weeks of mechanical thresholds on both paws (B) with significant decreases in the OBX group. Withdrawal frequency after an acetone drop is presented from both paws (C) at various time points before and after OBX. The AUC in the acetone test from the four weeks are shown in both paws (D) with significant increases in the OBX group. The withdrawal latency to a noxious mechanical stimulus is presented in both paws (E) with no differences between groups at the time points evaluated. The results are presented as mean ± SEM, n = 9–10 rats per group. The AUC in the pin prick test from the four weeks are shown in both paws (F). The results are presented as mean ± SEM, n = 9–10 rats per group. *p < 0.05, * *p < 0. 01, * **p < 0. 001 compared to the control group (sham rats). *Abbreviations: area under the curve, AUC; Olfactory bulbectomy, OBX.*

microglia in the BLA (Fig. 3H) ($p \leq 0.01$). Fig. S2 contains data broken down into left and right BLA.

Correlation was performed between behavior and the morphology or number of astrocytes in the BLA. The AUC mechanical threshold averaged from both paws (R^2 =0.934) correlated with the total filament length of GFAP-positive astrocytes in the BLA (Fig. 7A). The AUC of the response frequency after acetone administration averaged from both paws correlated with the number of GFAP-positive astrocytes (R^2 =0.8911) in the BLA (Fig. 7E) and with the total filament length (R^2 =0.9085) of Iba1-positive microglia in the BLA (Fig. 7K).

3.3. OBX increases the number and total filament length in GFAP-positive astrocytes and reduces the total filament in Iba1-positive microglia in the CeA

Our results indicate that compared to controls (sham animals), OBX disrupts the morphology of GFAP-positive astrocytes in the CeA. The results from the total CeA indicate that OBX increases the total filament length (Fig. 4A) ($p \leq 0.001$), arborization (Fig. 4B) [distance $F(1170) = 167.9$, $p \leq 0.001$; intersections $F(9170) = 89.36$, $p \leq 0.001$; Interaction $F(9, 170) = 7.319$, $p \leq 0.001$; distance from cell body 20–45 μm] and the number of order (Fig. 4C) [number $F(1153) = 65.43$, $p \leq 0.001$; filament length $F(8153) = 192.5$, $p \leq 0.001$; Interaction $F(8, 153) =$

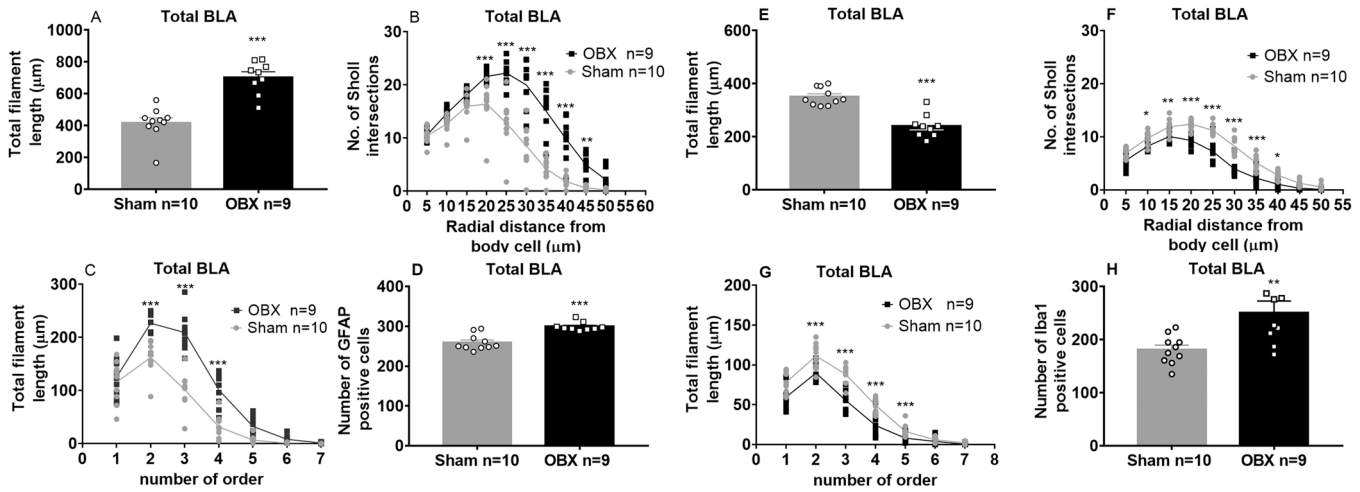

Fig. 3. OBX induces morphological and density alterations in GFAP-positive astrocytes and Iba1-positive microglia in the BLA in rats. Regarding glial morphology and number of GFAP or Iba1 positive cells, we evaluated and averaged the total number from both sides. OBX increases the total filament length (A), arborization (B) and the number of order (C) in GFAP-positive astrocytes in the BLA. The number of GFAP+ astrocytes is increased in the BLA (D) in tissue from OBX rats. OBX decreases the total filament length (E) arborization (F) and the number of order of (G) in Iba1-positive microglia in the BLA. The number of Iba1-positive microglia is increased in the BLA (H) in tissue from OBX rats. The results are presented as mean ± SEM, n = 9–10 rats per group. *p < 0.05, * *p < 0. 01, * **p < 0. 001 compared to the control group (sham rats). *Abbreviations: basolateral amygdala, BLA; glial fibrillary acidic protein, GFAP; ionizing calcium-binding adaptor molecule 1, Iba1; Olfactory bulbectomy, OBX.*

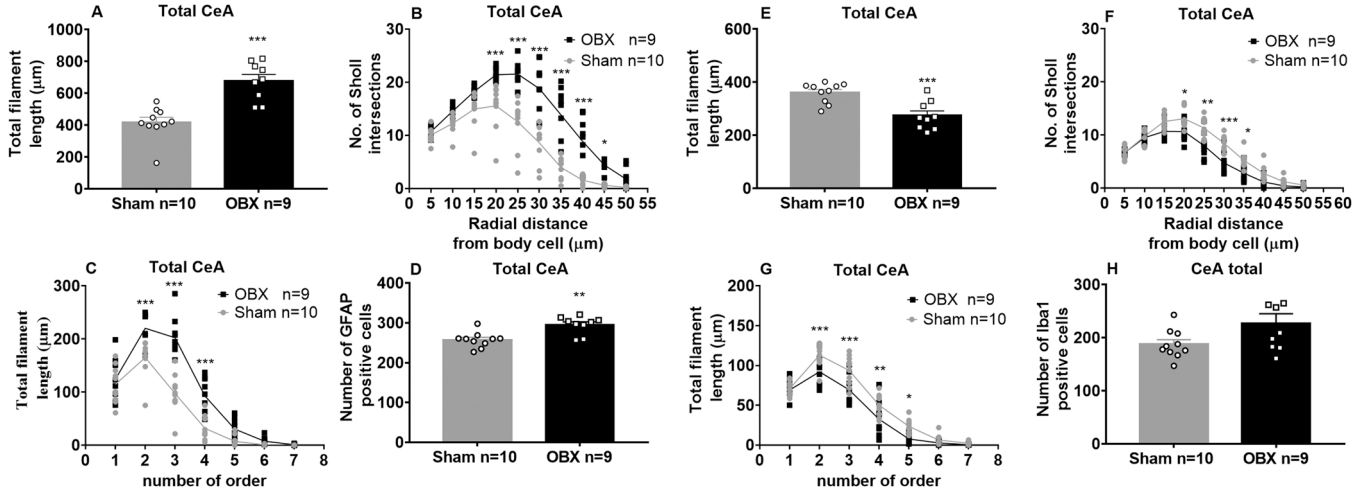

Fig. 4. OBX causes morphological and density alterations in GFAP-positive astrocytes and Iba1-positive microglia in the whole CeA in rats. Regarding glial morphology and number of GFAP or Iba1 positive cells, we evaluated and averaged the total number from both sides. OBX increases the total filament length (A) arborization (B) and the number of order (C) in GFAP-positive astrocytes in the CeA. The number of GFAP+ astrocytes was increased in the CeA (D) in tissue from OBX rats. OBX decreased the total filament length (E) arborization (F) and the number of order (G) in Iba1-positive microglia in the CeA. The number of Iba1-positive microglia remained similar between groups in the CeA (H). The results are presented as mean ± SEM, n = 9–10 rats per group. *p < 0.05, * *p < 0. 01, * **p < 0. 001 compared to the control group (sham rats). *Abbreviations: central amygdala, CeA; glial fibrillary acidic protein, GFAP; ionizing calcium-binding adaptor molecule 1, Iba1; Olfactory bulbectomy, OBX.*

11.62, $p \leq 0.001$; number of order 2–4] of GFAP-positive astrocytes. OBX increases the number of GFAP+ astrocytes in the whole CeA (Fig. 4D) ($p \leq 0.01$).

Regarding microglia, OBX decreased the total filament length (Fig. 4E) ($p \leq 0.001$), arborization (Fig. 4F) [distance $F(1170) = 65.2$, $p \leq 0.001$; intersections $F(9170) = 177.3$, $p \leq 0.001$; Interaction $F(9, 170) = 4.027$, $p \leq 0.001$; distance from cell body 20–35 μm] and the number of order (Fig. 4 G) [number $F(1153) = 32.04$, $p \leq 0.001$; filament length $F(8153) = 245$, $p \leq 0.001$; Interaction $F(8, 153) = 3.693$, $p \leq 0.001$; number of order 2–5] of Iba1-positive microglia in the CeA. Finally, OBX does not affect the number of Iba1-positive microglia in the whole CeA (Fig. 4H). Individual data from the left and right CeA are represented in Fig. S3.

Correlation was performed to test for a relationship between the behavior and the morphology or number of astrocytes in the CeA. The AUC of mean mechanical thresholds correlates with the total filament length ($R^2 = 0.9229$) of GFAP-positive astrocytes in the CeA (Fig. 7B). The AUC for mean mechanical thresholds correlates with the total filament length ($R^2 = 0.8856$) (Fig. 7G) and the number ($R^2 = 0.9078$) of Iba1-positive microglia in the CeA. (Fig. 7H). The AUC for average frequency of response to acetone correlates with the total filament length of Iba1-positive microglia ($R^2 = 0.9471$) in the CeA (Fig. 7L).

3.4. OBX increases the number and total filament length in GFAP-positive astrocytes and reduces the total filament length in Iba1-positive microglia in the CA1 subregion of the hippocampus

Our results indicate that compared to controls (sham animals), OBX disrupts the morphology of GFAP-positive astrocytes in the CA1. The data from the total CA1 indicates that OBX increases the total filament length (Fig. 5A) ($p \leq 0.001$), arborization (Fig. 5B) [distance $F(1170) = 192.2$, $p \leq 0.001$; intersections $F(9170) = 102.7$, $p \leq 0.001$; Interaction $F(9, 170) = 8.723$, $p \leq 0.001$; distance from cell body 20–45 μm] and the number of order (Fig. 5 C) [number $F(1153) = 68.93$, $p \leq 0.001$; filament length $F(8153) = 187.8$, $p \leq 0.001$; Interaction $F(8, 153) = 13.23$, $p \leq 0.001$; number of order 2–4] of GFAP-positive astrocytes. OBX also augments the number of GFAP-positive astrocytes in the CA1 (Fig. 5D). ($p \leq 0.001$).

Regarding microglia, OBX decreases the total filament length (Fig. 5E) ($p \leq 0.01$), with specific modifications in arborization (Fig. 5F) [distance $F(1170) = 38.39$, $p \leq 0.001$; intersections $F(9170) = 200.2$, $p \leq 0.001$; Interaction $F(9, 170) = 0.4968$, $p > 0.05$; distance from cell body 30 μm] and the number of order (Fig. 5G) [number $F(1153) = 16.78$, $p \leq 0.001$; filament length $F(8153) = 271.3$, $p \leq 0.001$; Interaction $F(8, 153) = 1.233$, $p > 0.05$; number of order 2] of Iba1-positive microglia in the CA1. Finally, OBX does not modulate the number of Iba1-positive microglia in the whole CA1 (Fig. 5H). Individual data from the left and right CA1 are represented in Fig. S4.

Correlation was performed to test for a relationship between behavior and the morphology or number of astrocytes in the CA1 subregion of the hippocampus. The AUC of average frequency after acetone administration correlates with the total filament length of GFAP-positive astrocytes in the CA1 hippocampus ($R^2 = 0.9093$) (Fig. 7F).

3.5. OBX reduces the total filament length and increases the number of Iba1-positive microglia in the PFC

Our results indicate that compared to controls (sham animals), OBX has minimal effects on the number and morphology of GFAP-positive astrocytes in the PFC. The results from the total PFC indicate that OBX does not affect the total filament length (Fig. 6A) or the arborization (Fig. 6B), but modifies the number of order (Fig. 6C) [number $F(1153) = 5.83$, $p \leq 0.05$; filament length $F(8153) = 253$, $p \leq 0.001$; Interaction $F(8, 153) = 2.281$, $p \leq 0.05$; number of order 2] of GFAP-positive astrocytes. OBX does not modify the number of GFAP+ astrocytes in the PFC (Fig. 6D).

Regarding microglia, OBX decreases the total filament length (Fig. 6E) ($p \leq 0.001$) and modifies the arborization [distance $F(1,17) = 50.81$, $p \leq 0.001$; intersections $F(10,170) = 514.6$, $p \leq 0.001$; Interaction $F(10, 170) = 4.124$, $p < 0.001$] (Fig. 6. F) the number of order (Fig. 6G) [number $F(1153) = 38.23$, $p \leq 0.001$; filament length $F(8153) = 332.6$, $p \leq 0.001$; Interaction $F(8, 153) = 9.043$, $p \leq 0.001$; number of order 2,3,5] in Iba1-positive microglia in the PFC. Finally, OBX increases the number of Iba1-positive microglia in the whole PFC (Fig. 6H). Individual data from the left and right PFC are represented in Fig. S5 Representative images of immunohistochemistry in Iba1-positive microglia (Fig. 8) and GFAP-positive astrocytes (Fig. 9) from all regions are presented.

Correlation was performed to test for a relationship between behavior and the morphology or number of astrocytes in the PFC. The AUC for averaged mechanical thresholds correlates with the total filament length ($R^2 = 0.9062$) (Fig. 7C) and the number ($R^2 = 0.9381$) of GFAP-positive astrocytes in the PFC (Fig. 7D) They also correlated with the total filament length ($R^2 = 0.9285$) (Fig. 7I) and number ($R^2 = 0.8856$) of Iba1-positive microglia in the PFC (Fig. 7J).

3.6. Evaluation of the number of Iba1-positive microglia and GFAP-positive astrocytes in the rostral-caudal axis

OBX increases the number of GFAP-positive astrocytes in the BLA at − 2.56 mm and − 2.12 mm from Bregma (Fig. 10A) [distance $F(1,17) = 28.59$, $p \leq 0.001$; surgery $F(3,51) = 5.291$., $p \leq 0.001$; Interaction $F(3, 51) = 5.035$, $p \leq 0.001$]. OBX increases the number of Iba1-positive microglia in the BLA relative to Bregma (Fig. 10E) [distance $F(1,17) = 9.154$, $p \leq 0.001$; surgery $F(3,51) = 1.323$., $p>0.05$; Interaction $F(3, 51) = 0.331$, $p > 0.05$]. OBX increases the number of GFAP-positive astrocytes in the CeA at the extremes measured. OBX has significant effects on the number of GFAP+ astrocytes in the CeA at − 2.56 mm and − 1.88 mm from Bregma (Fig. 10B) [distance $F(1,17) = 15.51$, $p \leq 0.001$; surgery $F(3,51) = 4.488$., $p \leq 0.001$; Interaction $F(3, 51) = 0.1188$, $p > 0.05$]. Regarding microglia, OBX does not affect the number of Iba1-positive microglia in the CeA at the locations evaluated (Fig. 10F). OBX increases the number of GFAP-positive astrocytes in the

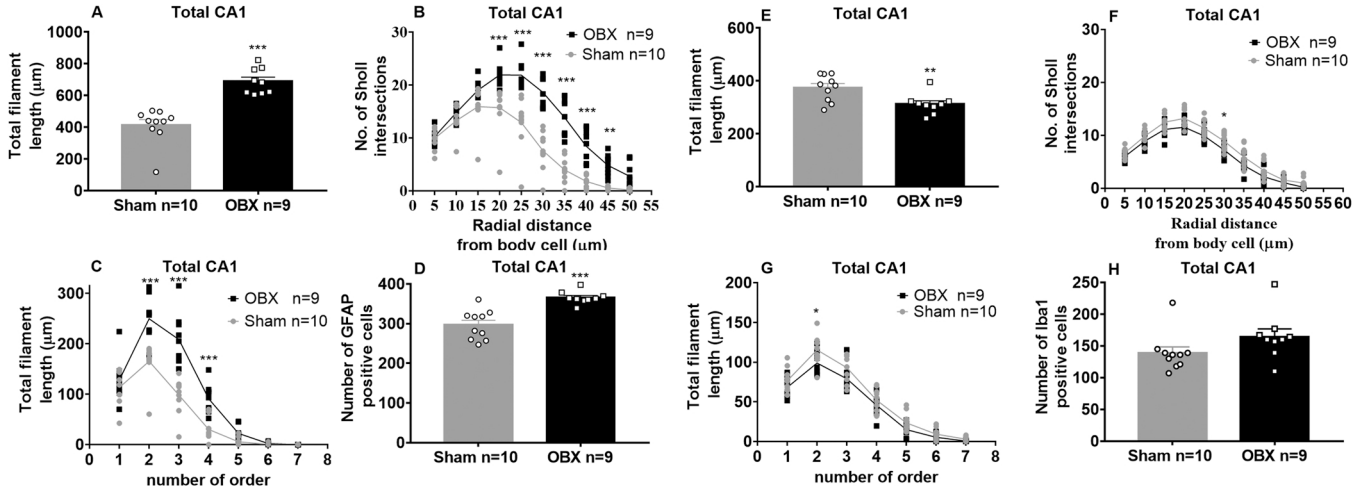

Fig. 5. OBX induced morphological and density alterations in GFAP-positive astrocytes and Iba1-positive microglia in the CA1 subregion of hippocampus in rats. Regarding glial morphology and number of GFAP or Iba1 positive cells, we evaluated and averaged the total number from both sides. OBX increased the total filament length (A) arborization (B) and the number of order (C) of GFAP-positive astrocytes in the CA1. The number of GFAP+ astrocytes was increased in the CA1 (D) in tissue from OBX rats. OBX decreased the total filament length (E) arborization (F) and the number of order (G) of Iba1-positive microglia in the CA1. The number of Iba1-positive microglia remained similar between groups in the CA1 (H). The results are presented as mean ± SEM, n = 9–10 rats per group. *$p < 0.05$, * *$p < 0.01$, * **$p < 0.001$ compared to the control group (sham rats). *Abbreviations: glial fibrillary acidic protein, GFAP; ionizing calcium-binding adaptor molecule 1, Iba1; Olfactory bulbectomy, OBX.*

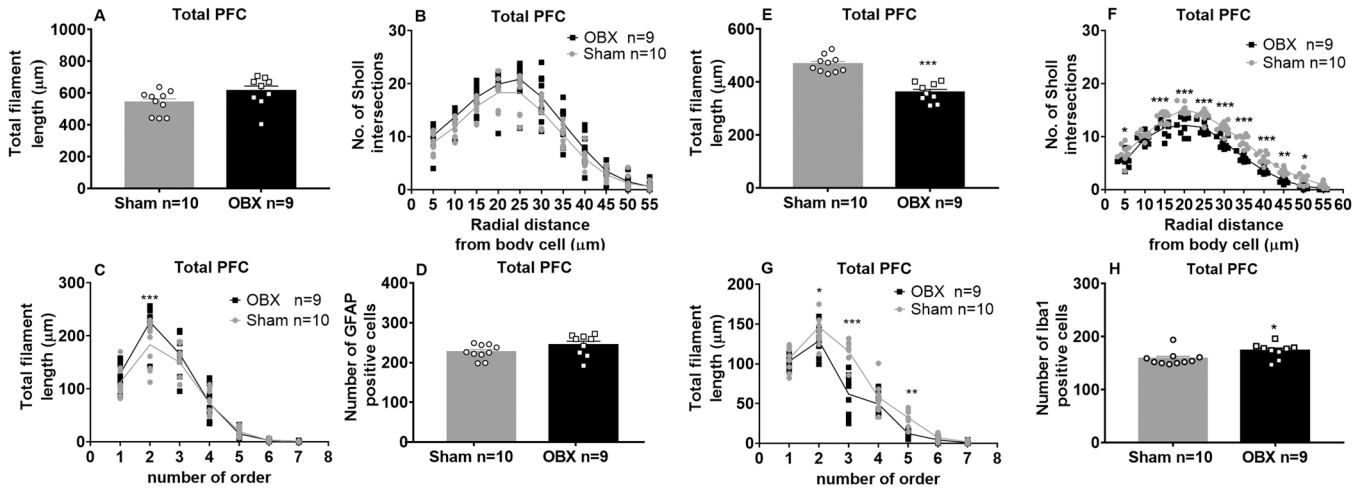

Fig. 6. OBX induced morphological and density alterations in GFAP-positive astrocytes and Iba1-positive microglia in the PFC in rats. Regarding glial morphology and number of GFAP or Iba1 positive cells, we evaluated and averaged the total number from both sides. OBX does not modify the total filament length (A) or arborization (B) of GFAP-positive astrocytes in the PFC. OBX increased the intersection in the second order (C) of GFAP-positive astrocytes in the PFC. The number of GFAP+ astrocytes remained unaffected in the whole PFC (D). OBX decreased the total filament length (E) arborization (F) and the number of order (G) of Iba1-positive microglia in the PFC. The number of Iba1-positive microglia is increased in the PFC in OBX rats (H). The results are presented as mean ± SEM, n = 9–10 rats per group. *p < 0.05, * *p < 0. 01, * **p < 0. 001 compared to the control group (sham rats). *Abbreviations: glial fibrillary acidic protein, GFAP; ionizing calcium-binding adaptor molecule 1, Iba1; Olfactory bulbectomy, OBX; prefrontal cortex, PFC.*

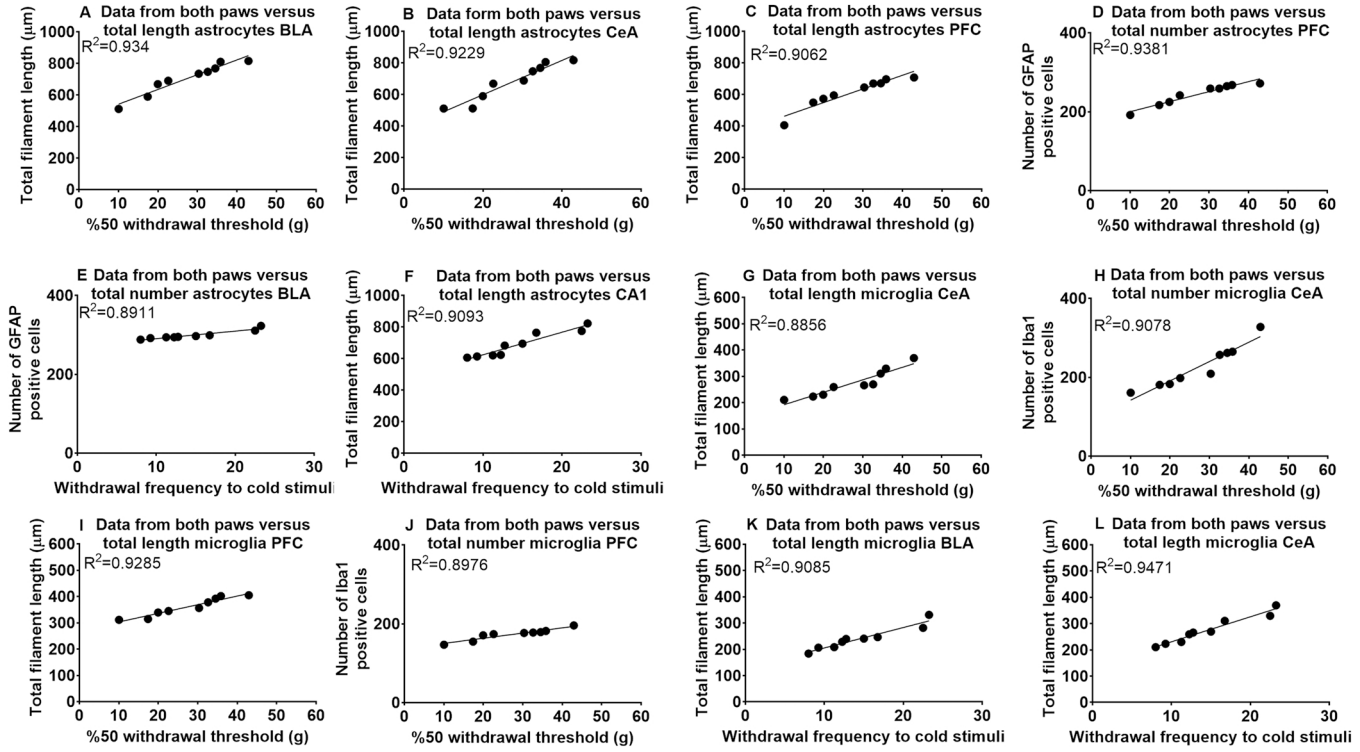

Fig. 7. Correlations between glial expression and behavioral assessment in rats. In this figure, linear regressions of correlations with at least a $R^2 \geq 0.88$ only in data from OBX rats. The AUC mechanical thresholds in both paws correlate with the total filament length in GFAP-positive astrocytes in the BLA (A). The AUC mechanical thresholds in both paws correlate with the total filament length in GFAP-positive astrocytes in the CeA (B). The AUC mechanical thresholds in both paws correlate with the total filament length in GFAP-positive astrocytes in the PFC (C). The AUC mechanical thresholds in both paws correlate with the total number in GFAP-positive astrocytes in the PFC (D). The AUC frequency after acetone administration in both paws correlates with the total number in GFAP-positive astrocytes in the BLA (E). The AUC frequency after acetone administration in both paws correlates with the total filament length of GFAP-positive astrocytes in the CA1 (F). The AUC mechanical thresholds in both paws correlate with the total filament length in Iba1-positive microglia in the CeA (G). The AUC mechanical thresholds in both paws correlate with the total number in Iba1-positive microglia in the CeA (H). The AUC mechanical thresholds in both paws correlate with the total filament length of Iba1-positive microglia in the PFC (I). The AUC mechanical thresholds in both paws correlate with the total number of Iba1-positive microglia in the PFC (J). The AUC frequency after acetone administration in both paws correlates with the total filament length in Iba1-positive microglia in the BLA (K). The AUC frequency after acetone administration in both paws correlates with the total filament length of Iba1-positive microglia in the CeA (L). *Abbreviations: basolateral amygdala, BLA; central amygdala, CeA; glial fibrillary acidic protein, GFAP; ionizing calcium-binding adaptor molecule 1, Iba1; Olfactory bulbectomy, OBX; prefrontal cortex, PFC.*

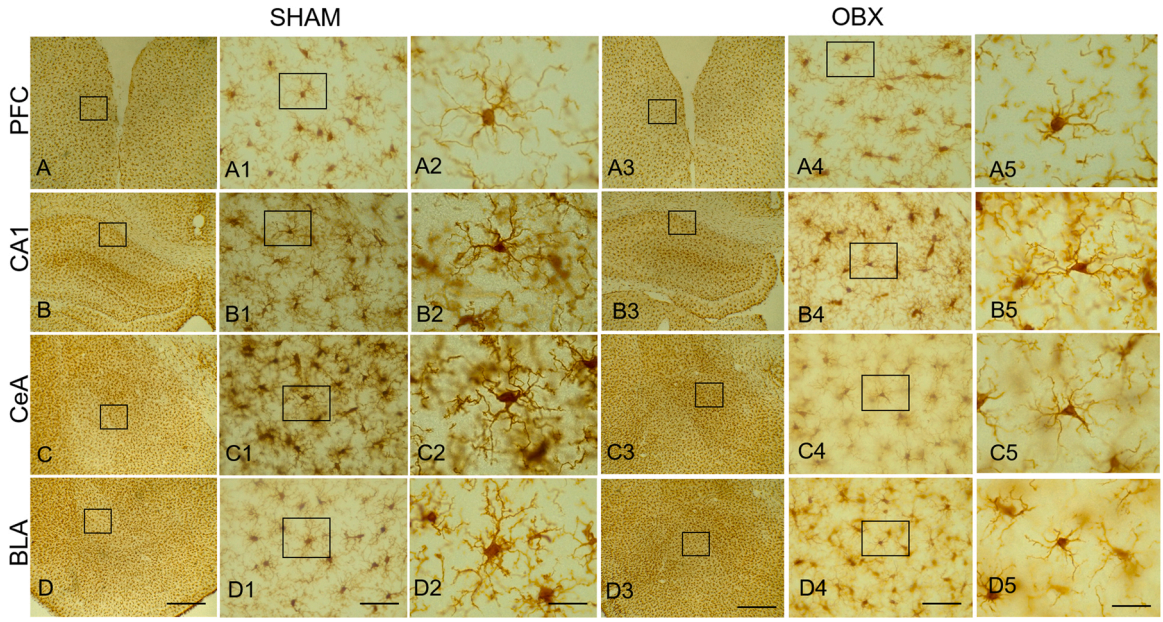

Fig. 8. Representative examples of Iba1-positive microglia in all regions evaluated. Images from A to D and A3 to D3 were taken at 4X magnification from sham animals. Images from A1 to D1 and A4 to D4 were taken at 40X magnification. Images from A2-D2 and A5-D5 are taken from the adjacent figure at 100X magnification. Scale bar in A-D and A3-D3 = 500 μm, A1-D1 and A4-D4 = 50 μm, A2-D2 and A5-D5 = 20 μm. *Abbreviations: basolateral amygdala, BLA; central amygdala, CeA; glial fibrillary acidic protein, GFAP; ionizing calcium-binding adaptor molecule 1, Iba1; Olfactory bulbectomy, OBX; prefrontal cortex, PFC.*

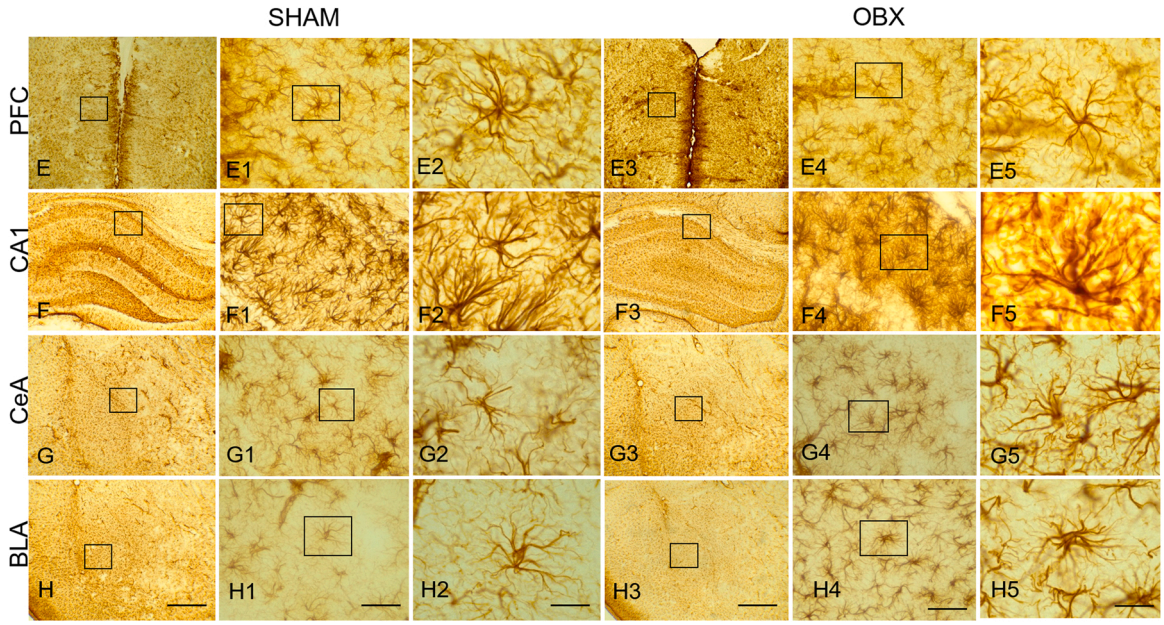

Fig. 9. Representative examples of GFAP-positive astrocytes in all regions evaluated. Images from E to H and E3 to H3 were taken at 4X magnification from sham animals. Images from E1 to H1 and E4 to H4 were taken at 40X magnification. Images from E2-H2 and E5-H5 are taken from the adjacent figure at 100X magnification. Scale bar in E-H and E3-H3 = 500 μm, E1-H1 and E4-H4 = 50 μm, E2-H2 and E5-H5 = 20 μm. *Abbreviations: basolateral amygdala, BLA; central amygdala, CeA; glial fibrillary acidic protein, GFAP; ionizing calcium-binding adaptor molecule 1, Iba1; Olfactory bulbectomy, OBX; prefrontal cortex, PFC.*

CA1 in all points evaluated, − 3.14 mm to − 2.3 mm distance from Bregma [distance $F(1,17)= 26.32$, $p \leq 0.001$; surgery $F(3,51)= 0.7591.$, $p > 0.05$; Interaction $F(3, 51)= 1.681$, $p > 0.05$] (Fig. 10C) but did not change the number of astrocytes in the PFC in any of the points evaluated (Fig. 10D). Regarding microglia, OBX does not affect the number of Iba1-positive microglia in the CA1(Fig. 10G) or the PFC (Fig. 10H) at any point evaluated.

4. Discussion

The present study shows that following OBX, rats exhibit behavioral and glial signs often seen in MDD. OBX reduces the magnitude of the stimulus necessary to evoke a mechanical withdrawal response. Moreover, while astrocytes showed increased number and hypertrophy, microglia showed the opposite, hypotrophy, in the same brain regions suggesting glial activation in the CNS after OBX.

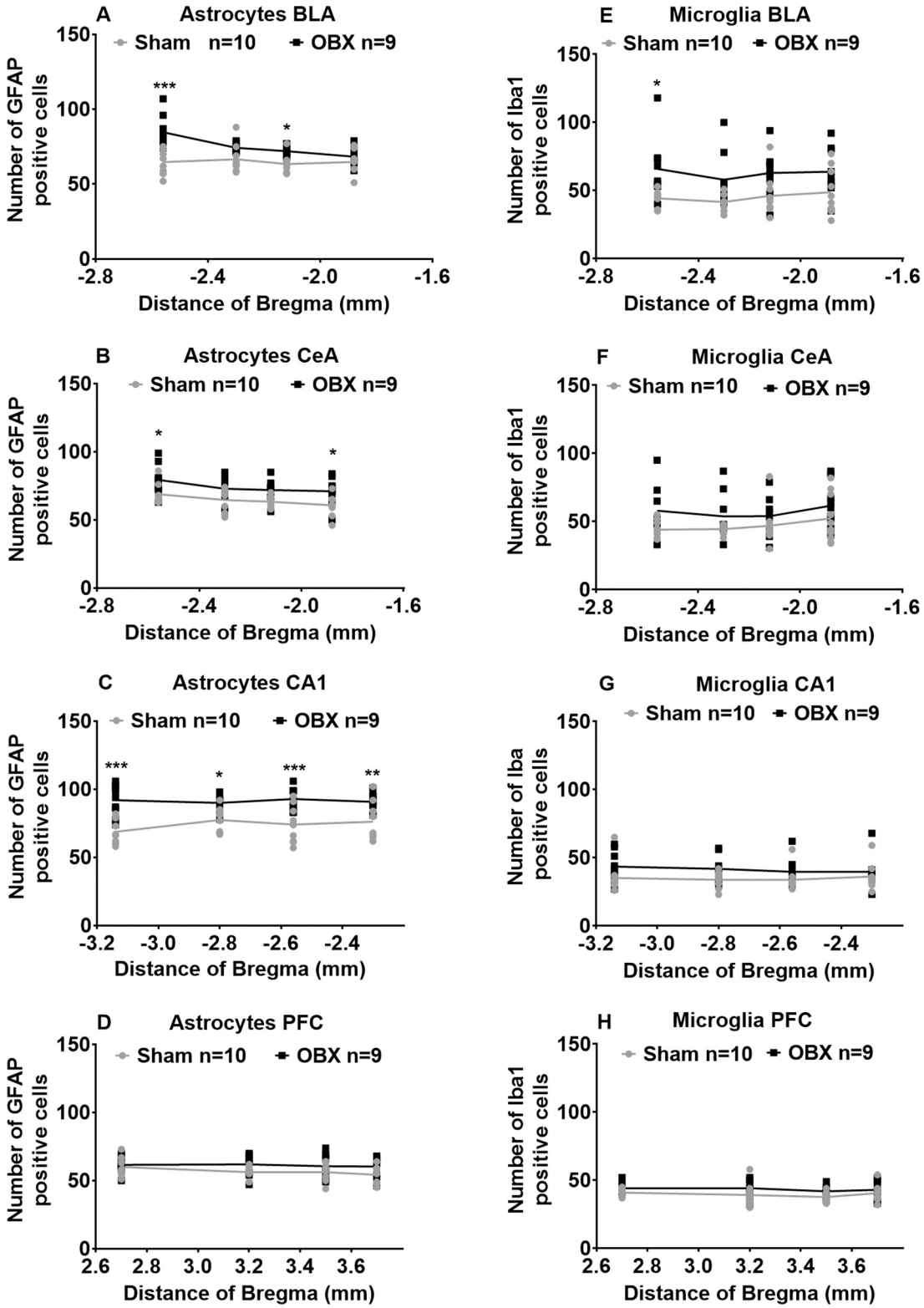

Fig. 10. The modifications in number of Iba1-positive microglia and GFAP-positive astrocytes are not homogeneous in the rostral-caudal axis in OBX rats. The number of GFAP-positive astrocytes is increased at − 2.56 and − 2.12 mm from Bregma in the BLA (A) in tissue from OBX rats. The number of GFAP-positive astrocytes is increased at − 2.56 and − 1.88 mm from Bregma in the CeA (B) in OBX rats. The number of GFAP-positive astrocytes is increased from − 3.14 to − 2.30 mm distance from Bregma in the CA1 (C) from OBX rats. The number of GFAP-positive astrocytes remained unaffected in the PFC (D). The number of Iba1-positive microglia is increased selectively at − 2.56 from distance of Bregma in the BLA (E) in tissue from OBX rats. The number of Iba1-positive microglia remained similar between groups from − 2.56 to − 1.88 mm distance from Bregma in the CeA (F). The number of Iba1-positive microglia remained similar between groups from − 3.14 to − 2.30 mm distance from Bregma in CA1 (G). The number of Iba1-positive microglia remained similar between groups from 3.70 to − 2.70 mm distance from Bregma in the PFC (H) between groups.

4.1. OBX induces long-lasting mechanical and thermal (cold) allodynia

To the best of our knowledge, this is the first study to evaluate nociceptive assays at multiple time points in this animal model of depression. Most data read-outs in studies of OBX rats are collected between 3 and 4 weeks following surgery (Kelly et al., 1997; Morales-Medina et al., 2017). Our present results show that OBX induces two types of allodynia: mechanical and cold. In apparent agreement, rats displayed mechanical allodynia fifteen days following OBX surgery (Belcheva et al., 2009). Moreover, OBX rats presented mechanical and thermal (cold) allodynia without thermal (heat) hyperalgesia two (Burke et al., 2013) and three weeks following surgery (Burke et al., 2015). In clear contrast, Wang et al. (2010) observed thermal (heat) hyperalgesia and an exacerbated response to formalin three weeks after OBX in rats.

It is of interest to note that the peripheral allodynia in this model is caused by an alteration in the CNS. Early on, various researchers observed pain responses after CNS manipulations in the absence of injury. For example, Kolber et al. (2010) showed that activation of the amygdala could induce mechanical allodynia of the paw. Moreover, formalin-induced allodynia in the paw is reduced after BLA deactivation (Carrasquillo & Gereau, 2007). In addition, intracerebroventricular administration of interleukin-6 (IL-6) reduced heat paw-withdrawal latency (thermal hyperalgesia) (Oka et al., 1995). In particular, increased levels of TNF-α in the hippocampus drove thermal hyperalgesia and mechanical allodynia in the rat hind paws (Martuscello et al., 2012). In the following sections, we will discuss the brain regions as well as the glial processes implicated in pain-like behaviors.

4.2. OBX modifies the density and organization of processes in astrocytes and microglia in several brain regions

Clinical and preclinical data indicate the involvement of the PFC, BLA and hippocampus in mood-related disorders (Morales-Medina et al., 2017). Consolidated and emerging data also show the involvement of these regions in nociceptive behaviors. For example, the amygdala comprises several nuclei including the BLA and CeA and is involved in emotional as well as nociceptive processing (Baas et al., 2004; Goncalves et al., 2008). Of note, while the BLA receives nociceptive inputs from the hypothalamus and cortex, the CeA receives its information from the parabrachial nucleus (LeDoux et al., 1990; Bernard et al., 1993). Furthermore, increased levels of TNF-α in the hippocampus induce pain-like behaviors in the hind paws (Martuscello et al., 2012). Among the regions studied, the PFC is the least studied brain region regarding nociception. For example, transcranial stimulation of the PFC induced analgesic effects in a mouse model of neuropathic pain (Gan et al., 2021). Therefore, these three brain regions are involved in emotional and nociceptive processes.

Glia are the most abundant cells in the CNS. In particular, astrocytes and microglia have been implicated in MDD (Si et al., 2004; Hercher et al., 2009; Torres-Platas et al., 2016). Astrocytes are the most common glial cells within the CNS and liberate neurotrophic factors and neurotransmitters in the synaptic cleft (Dolotov et al., 2022). One mature astrocyte can interact with 300–600 neuronal dendrites in a rodent brain, making them quite relevant (Halassa et al., 2007). In addition, microglia are the resident immune cells that represent 10–15% of the CNS cells that modulate neuroinflammatory molecules (Kettenmann et al., 2011; Yanguas-Casas et al., 2020). In pathological conditions, glial cells become activated; astrocytes increase the length of their processes and microglia increase their body size and decrease their process length (amoeba state) (Lenz et al., 2013; Yanguas-Casas et al., 2020; Dolotov et al., 2022). In the current study, we observed an increase in the number of astrocytes and their process length in the BLA, CeA and CA1 of the hippocampus. Moreover, in all regions evaluated microglial process numbers were reduced, except in the BLA and PFC where their numbers were increased. Previously, and in apparent agreement, Burke et al. (2013) observed an increase in GFAP and CD11b (microglia) mRNA in the amygdala 22 days after OBX. However, post-transcriptional modifications could occur prior to protein maturation. Keilhoff et al. (2006) noted that OBX increased the number of 5-bromo-2´-deoxy-uridine positive cells, a marker of proliferation, in the BLA. This process could be a plastic compensatory modification. In the frontal cortex in OBX mice, Machado et al. (2020) found higher expression of GFAP density, which might be related to the increased number of astrocytes seen in the current study. Almeida et al. (2021) recently noted altered levels of interleukins (IL), glial-related cytokines, in the hippocampus of OBX mice. For instance, OBX raised the expression of IL-1, IL-6, and tumor necrosis factor α and decreased the levels of IL-10, which may be related to the glial abnormalities in the hippocampus reported in the current study. In addition, 42 days after surgery, astrocyte numbers and processes increase in the hippocampus of OBX mice (Takahashi et al., 2018), similar to the results presented in this study. Takahashi et al. (2018) also observed an increase in processes and number in Iba1-positive microglial cells in the hippocampus, which is in contrast to the findings of the current investigation. As such, discrepancies between results may be due to methodology as they may be influenced by factors like species, length of recovery after surgery, and other manipulations. Other approaches have evaluated the expression or number of astrocytes and microglia in other models of depression-related behavior. For example, chronic restrain stress (CRS) for 10 days reduced the density of astrocytes with increased length of astrocytic processes in the BLA with no modification in the CA3 region of the hippocampus (Naskar & Chattarji, 2019). Moreover, chronic stress reduced the astrocytic processes in various layers of the PFC and the number of GFAP-positive cells in rats (Tynan et al., 2013). Similarly, chronic stress reduces the astrocytic processes in the PFC in mice (Codeluppi et al., 2021). In addition, CRS for 21 days increased the number of microglia with increased expression of IL-10 and TNF-α in the rat hippocampus (Chen et al., 2022a). Learned helplessness in mice, a model of depression-related behavior, increases the number of microglia in the dentate gyrus of the hippocampus (Worthen et al., 2020). Chronic unpredictable stress results in an increased number of microglia in the CA1/CA3 and dentate gyrus of the hippocampus in rats (Xiao et al., 2021). Repeated social defeat stress elicits an increased number of microglia in the basal nucleus of the BLA in rats (Munshi et al., 2020). As shown, previous studies typically only evaluated a single population of glial cells while the current study measures two important populations of glial cells in the same animal. In the present study, we observed that both types of glial cells are activated in the BLA, CeA and CA1 subregions of the hippocampus. In the PFC, there was a retraction of microglial processes (microglial activation) with reduced numbers of astrocytes, suggesting a plastic modification. Of note and to the best of our knowledge, we are the first group to show microglial/astrocytic alterations in the CeA in a rat model of depression.

Although there is general agreement that glia are important in MDD, the findings vary by area (Miller & Raison, 2016; Wohleb et al., 2016). Furthermore, early research on MDD patients´ brain regions focused on cortical and hippocampal areas. Stockmeier et al. (2004) showed an increase in glial density in the CA1/dentate gyrus of the hippocampus from subjects with MDD, but the groundbreaking study of Ongur et al. (1998) noted a drop in the number of glial cells in the PFC. Because Nissl labelling was utilized in both studies, it was impossible for the authors to say whether the alterations were present in astrocytes or microglia. Later, Cotter et al. (2001) used cresyl violet staining to detect a decrease in glial cell density in the ACC. Once more, the authors were unable to specify the kind of glial cell that was being examined. Additionally, by using Golgi staining, Torres-Platas et al. (2011) observed astrocytic hypertrophy in the ACC. In a different method, Si et al. (2004) noticed a decrease in GFAP expression in the PFC in tissue from MDD patients. Moreover, according to Cobb et al. (2016), the density of GFAP-positive astrocytes is reduced in the hippocampus. Zhang et al. (2021) recently discovered changes in astrocytic gene expression in the PFC from tissue

from MDD patients. Although there has been a definitive advancement in our understanding of glial changes in MDD, there are still certain limitations, such as the use of antidepressant medications and lateralized and small sample sizes. Moreover, to the best of our knowledge there are no data on glia in the BLA or CeA in tissue from MDD patients. Moreover, Rajkumar and Dawe (2018) presented an insightful review displaying the abnormalities presented in the PFC between the OBX model and MDD, therefore, this work adds relevant information in this matter. Moreover, the current results thus provide translational information by presenting novel new brain regions to be assessed in MDD, the comorbidity of MDD and pain and the changes in both the quantity and morphology of two important CNS glial cells.

4.3. Glial activation in the CNS and its association with pain

While activation of astrocytes and microglia are recognized as key participants in rodent models of pain (Ikeda et al., 2012), their involvement is not completely understood. Moreover, typical models of pain are framed after injury or inflammatory agent administration in the dorsal horn or periphery with local measurements. More recent approaches evaluate CNS-related effects (Morales-Medina et al., 2020; Cooper et al., 2022). There is much evidence regarding glial effects on the brain. Unilateral constriction of the infraorbital nerve, an animal model of neuralgia, activates microglia in the hippocampus (ipsilateral side) and induces anxiodepressive-related behaviors (Chen et al., 2022b). In addition, water avoidance stress induces visceral hypersensitivity accompanied by microglial activation in the CeA in rats (Yuan et al., 2020). Moreover, streptozotocin-induced diabetes results in peripheral mechanical allodynia accompanied by activation of astrocytes in the BLA (Lu et al., 2022). More interesting is the fact that inhibition of astrocytes in the BLA dramatically reduces streptozotocin-induced mechanical allodynia (Lu et al., 2022). Recently, a model of cancer-induced pain shows activated microglia in the BLA in mice (Jiang et al., 2022). In this regard, our current study shows correlations between glial alterations and the behavioral deficits observed, further suggesting the involvement of glia in these brain regions as key components of nociceptive processes.

While the mechanism(s) by which glia modify emotional and nociceptive process is not fully understood, critical information is shedding light on this matter. Astrocytes and microglia are structural components of the so-called quad-partite synapse along with pre- and post-synaptic endings of neurons (Schafer et al., 2013), therefore these cells participate with numerous molecules to induce neuroplasticity. Moreover, administration of glial-induced molecules such as IL-6 (Oka et al., 1995) or TNF-α (Martuscello et al., 2012) to the CNS are capable of eliciting pain-related behaviors in the extremities. Astrocyte-related neurotransmitters including glutamate, γ-aminobutyric acid, dopamine or norepinephrine could also induce plastic modifications in the neurons (Canul-Tec et al., 2022) resulting in nociceptive alterations. In addition, glial products including brain-derived neurotrophic factor, fibroblast growth factor, nerve growth factors, and glial-derived neurotrophic factor regulate the function and plasticity of neurons (Poyhonen et al., 2019) also modifying nociception.

4.4. OBX induces asymmetric behavioral effects

Numerous studies have documented hemispheric lateralization of emotional and nociceptive processes in various brain regions including the PFC and amygdala (Phelps & LeDoux, 2005; Ji & Neugebauer, 2009; Yoshimura et al., 2009). In the current study, the behavioral results indicate an asynchrony in the appearance of symptoms in the extremities. While mechanical allodynia is observed first on the right paw, thermal allodynia is presented first in the left extremity. At the end of the study, we observed that the number of microglial cells is increased in the left side of the CeA, the same was observed in the PFC right side. At the moment, we do not know if the activation of microglial cells was homogeneous but at four weeks post injury, we observed lateralized effects. Previously, Kolber et al. (2010) observed that while neural activation in the left BLA induced contra-lateral mechanical allodynia in the paw, left neural activation resulted in mechanical allodynia in both paws suggesting hemispheric lateralization of the BLA (Kolber et al., 2010). In addition, Ji and Neugebauer (2009) observed that the right CeA displays bigger receptive fields compared to the left CeA in absence of injury in rats. Moreover, in a rat model of arthritis, neurons in the right CeA developed increased responsiveness and the authors suggested an asymmetric output from this region to target nuclei (Ji & Neugebauer, 2009).

5. Conclusions

The current data suggest that OBX induces nociceptive alterations that appear asynchronously, reinforcing the idea of comorbidity between pain and depression. Moreover, the behavioral deficits observed in this animal model of depression are accompanied by glial alterations, further supporting the neuroinflammatory hypothesis of depression.

Acknowledgments

JCMM and GF recognize the National Research System of Mexico (CONACyT) for membership. GGP thanks CONACyT for scholarship (No. 756443). This research received no specific grant from any funding agency in the public, commercial or non-profit sectors. This work was funded by CINVESTAV. Thanks to Renée Donahue for editing and proofreading the document.

Conflict-of-interest statement

The authors have no known conflicts of interest in regards to the materials discussed in this manuscript.

Appendix A. Supporting information

Supplementary data associated with this article can be found in the online version at doi:10.1016/j.ibneur.2023.05.006.

References

Almeida, R.F., Ganzella, M., Machado, D.G., Loureiro, S.O., Leffa, D., Quincozes-Santos, A., Pettenuzzo, L.F., Duarte, M., Duarte, T., Souza, D.O., 2017. Olfactory bulbectomy in mice triggers transient and long-lasting behavioral impairments and biochemical hippocampal disturbances. Prog. neuro-Psychopharmacol. Biol. Psychiatry 76, 1–11.

Almeida, R.F., Nonose, Y., Ganzella, M., Loureiro, S.O., Rocha, A., Machado, D.G., Bellaver, B., Fontella, F.U., Leffa, D.T., Pettenuzzo, L.F., Venturin, G.T., Greggio, S., da Costa, J.C., Zimmer, E.R., Elisabetsky, E., Souza, D.O., 2021. Antidepressant-Like Effects of Chronic Guanosine in the Olfactory Bulbectomy Mouse Model. Front. Psychiatry 12, 701408.

Baas, D., Aleman, A., Kahn, R.S., 2004. Lateralization of amygdala activation: a systematic review of functional neuroimaging studies. Brain Res. Brain Res. Rev. 45, 96–103.

Bautista-Carro, M.A., Flores, G., Iannitti, T., Galindo-Paredes, G., Morales-Medina, J.C., 2021. Curcuma longa Administration Significantly Reduces Acute and Persistent Inflammatory Pain Measures in Male and Female Rats. Arch. Vet. Sci. Med 4, 24–33.

Belcheva, I., Ivanova, M., Tashev, R., Belcheva, S., 2009. Differential involvement of hippocampal vasoactive intestinal peptide in nociception of rats with a model of depression. Peptides 30, 1497–1501.

Bernard, J.F., Alden, M., Besson, J.M., 1993. The organization of the efferent projections from the pontine parabrachial area to the amygdaloid complex: a Phaseolus vulgaris leucoagglutinin (PHA-L) study in the rat. J. Comp. Neurol. 329, 201–229.

Burke, N.N., Finn, D.P., Roche, M., 2015. Chronic administration of amitriptyline differentially alters neuropathic pain-related behaviour in the presence and absence of a depressive-like phenotype. Behav. brain Res. 278, 193–201.

Burke, N.N., Geoghegan, E., Kerr, D.M., Moriarty, O., Finn, D.P., Roche, M., 2013. Altered neuropathic pain behaviour in a rat model of depression is associated with changes in inflammatory gene expression in the amygdala. Genes Brain Behav. 12, 705–713.

Canul-Tec, J.C., Kumar, A., Dhenin, J., Assal, R., Legrand, P., Rey, M., Chamot-Rooke, J., Reyes, N., 2022. The ion-coupling mechanism of human excitatory amino acid transporters. EMBO J. 41, e108341.

Carrasquillo, Y. & Gereau, R.Wt (2007) Activation of the extracellular signal-regulated kinase in the amygdala modulates pain perception. The Journal of neuroscience: the official journal of the Society for Neuroscience, 27, 1543–1551.
Carroll, L.J., Cassidy, J.D., Cote, P., 2004. Depression as a risk factor for onset of an episode of troublesome neck and low back pain. Pain 107, 134–139.
Chaplan, S.R., Bach, F.W., Pogrel, J.W., Chung, J.M., Yaksh, T.L., 1994. Quantitative assessment of tactile allodynia in the rat paw. J. Neurosci. Methods 53, 55–63.
Chen, L., Jiang, H., Bao, T., Wang, Y., Meng, H., Sun, Y., Liu, P., Quan, S., Li, W., Qi, S., Ren, X., 2022a. Acupuncture Ameliorates Depressive Behaviors by Modulating the Expression of Hippocampal Iba-1 and HMGB1 in Rats Exposed to Chronic Restraint Stress. Front. Psychiatry 13, 903004.
Chen, L.Q., Lv, X.J., Guo, Q.H., Lv, S.S., Lv, N., Xu, W.D., Yu, J., Zhang, Y.Q., 2022b. Asymmetric activation of microglia in the hippocampus drives anxiodepressive consequences of trigeminal neuralgia in rodents. Br. J. Pharmacol.
Cobb, J.A., O'Neill, K., Milner, J., Mahajan, G.J., Lawrence, T.J., May, W.L., Miguel-Hidalgo, J., Rajkowska, G., Stockmeier, C.A., 2016. Density of GFAP-immunoreactive astrocytes is decreased in left hippocampi in major depressive disorder. Neuroscience 316, 209–220.
Codeluppi, S.A., Chatterjee, D., Prevot, T.D., Bansal, Y., Misquitta, K.A., Sibille, E., Banasr, M., 2021. Chronic Stress Alters Astrocyte Morphology in Mouse Prefrontal Cortex. Int J. Neuropsychopharmacol. 24, 842–853.
Cooper, A.H., Hedden, N.S., Corder, G., Lamerand, S.R., Donahue, R.R., Morales-Medina, J.C., Selan, L., Prasoon, P., Taylor, B.K., 2022. Endogenous micro-opioid receptor activity in the lateral and capsular subdivisions of the right central nucleus of the amygdala prevents chronic postoperative pain. J. Neurosci. Res. 100, 48–65.
Cotter, D., Mackay, D., Landau, S., Kerwin, R., Everall, I., 2001. Reduced glial cell density and neuronal size in the anterior cingulate cortex in major depressive disorder. Arch. Gen. Psychiatry 58, 545–553.
Doan, L., Manders, T., Wang, J., 2015. Neuroplasticity underlying the comorbidity of pain and depression. Neural Plast. 2015, 504691.
Dolotov, O.V., Inozemtseva, L.S., Myasoedov, N.F., Grivennikov, I.A., 2022. Stress-Induced Depression and Alzheimer's Disease: Focus on Astrocytes. Int. J. Mol. Sci. **23**.
Fishbain, D.A., Cutler, R., Rosomoff, H.L., Rosomoff, R.S., 1997. Chronic pain-associated depression: antecedent or consequence of chronic pain? A review. Clin. J. Pain. 13, 116–137.
Gan, Z., Li, H., Naser, P.V., Han, Y., Tan, L.L., Oswald, M.J., Kuner, R., 2021. Repetitive non-invasive prefrontal stimulation reverses neuropathic pain via neural remodelling in mice. Prog. Neurobiol. 201, 102009.
Goncalves, L., Silva, R., Pinto-Ribeiro, F., Pego, J.M., Bessa, J.M., Pertovaara, A., Sousa, N., Almeida, A., 2008. Neuropathic pain is associated with depressive behaviour and induces neuroplasticity in the amygdala of the rat. Exp. Neurol. 213, 48–56.
Gonzalez-Granillo, A.E., Gnecco, D., Diaz, A., Garces-Ramirez, L., de la Cruz, F., Juarez, I., Morales-Medina, J.C., Flores, G., 2022. Curcumin induces cortico-hippocampal neuronal reshaping and memory improvements in aged mice. J. Chem. Neuroanat. 121, 102091.
Halassa, M.M., Fellin, T., Takano, H., Dong, J.H. & Haydon, P.G. (2007) Synaptic islands defined by the territory of a single astrocyte. The Journal of neuroscience: the official journal of the Society for Neuroscience, 27, 6473–6477.
Hanson, S. & Abbafati, C. & Aerts, J.G. & Al-Aly, Z. & Ashbaugh, C. & Ballouz, T. & Blyuss, O. & Bobkova, P. & Bonsel, G. & Borzakova, S. & Buonsenso, D. & Butnaru, D. & Carter, A. & Chu, H. & De Rose, C. & Diab, M.M. & Ekbom, E. & El Tantawi, M. & Fomin, V. & Frithiof, R. & Gamirova, A. & Glybochko, P.V. & Haagsma, J.A. & Haghjooy Javanmard, S. & Hamilton, E.B. & Harris, G. & Heijenbrok-Kal, M.H. & Helbok, R. & Hellemons, M.E. & Hillus, D. & Huijts, S.M. & Hultstrom, M. & Jassat, W. & Kurth, F. & Larsson, I.M. & Lipcsey, M. & Liu, C. & Loflin, C.D. & Malinovschi, A. & Mao, W. & Mazankova, L. & McCulloch, D. & Menges, D. & Mohammadifard, N. & Munblit, D. & Nekliudov, N.A. & Ogbuoji, O. & Osmanov, I.M. & Penalvo, J.L. & Petersen, M.S. & Puhan, M.A. & Rahman, M. & Rass, V. & Reinig, N. & Ribbers, G.M. & Ricchiuto, A. & Rubertsson, S. & Samitova, E. & Sarrafzadegan, N. & Shikhaleva, A. & Simpson, K.E. & Sinatti, D. & Soriano, J.B. & Spiridonova, E. & Steinbeis, F. & Svistunov, A.A. & Valentini, P. & van de Water, B.J. & van den Berg-Emons, R. & Wallin, E. & Witzenrath, M. & Wu, Y. & Xu, H. & Zoller, T. & Adolph, C. & Albright, J. & Amlag, J.O. & Aravkin, A.Y. & Bang-Jensen, B.L. & Bisignano, C. & Castellano, R. & Castro, E. & Chakrabarti, S. & Collins, J.K. & Dai, X. & Daoud, F. & Dapper, C. & Deen, A. & Duncan, B.B. & Erickson, M. & Ewald, S.B. & Ferrari, A.J. & Flaxman, A. D. & Fullman, N. & Gamkrelidze, A. & Giles, J.R. & Guo, G. & Hay, S.I. & He, J. & Helak, M. & Hulland, E.N. & Kereselidze, M. & Krohn, K.J. & Lazzar-Atwood, A. & Lindstrom, A. & Lozano, R. & Malta, D.C. & Mansson, J. & Mantilla Herrera, A.M. & Mokdad, A.H. & Monasta, L. & Nomura, S. & Pasovic, M. & Pigott, D.M. & Reiner, R. C., Jr. & Reinke, G.. & Ribeiro, A.L.P.. & Santomauro, D.F.. & Sholokhov, A.. & Spurlock, E.E.. & Walcott, R.. & Walker, A.. & Wiysonge, C.S.. & Zheng, P.. & Bettger, J.P.. & Murray, C.J.L.. & Vos, T.. (2022) Estimated Global Proportions of Individuals With Persistent Fatigue, Cognitive, and Respiratory Symptom Clusters Following Symptomatic COVID-19 in 2020 and 2021. JAMA: the journal of the American Medical Association, 328, 1604–1615.
☑Hercher, C., Turecki, G., Mechawar, N., 2009. Through the looking glass: examining neuroanatomical evidence for cellular alterations in major depression. J. Psychiatr. Res. 43, 947–961.
Ikeda, H., Kiritoshi, T., Murase, K., 2012. Contribution of microglia and astrocytes to the central sensitization, inflammatory and neuropathic pain in the juvenile rat. Mol. Pain. 8, 43.
Jesulola, E., Micalos, P., Baguley, I.J., 2018. Understanding the pathophysiology of depression: From monoamines to the neurogenesis hypothesis model - are we there yet? Behav. Brain Res. 341, 79–90.
Ji, G., Neugebauer, V., 2009. Hemispheric lateralization of pain processing by amygdala neurons. J. Neurophysiol. 102, 2253–2264.
Jiang, L., Hao, J., Yang, X.L., Zhu, J.X., Wang, Y., Huang, Y.L., Sun, Y.E., Mao, Y.T., Ni, K., Gu, X.P., Ma, Z.L., 2022. Basolateral Amygdala Reactive Microglia May Contribute to Synaptic Impairment and Depressive-Like Behavior in Mice with Bone Cancer Pain. Neurochem. Res. 47, 3454–3463.
Keilhoff, G., Becker, A., Grecksch, G., Bernstein, H.G., Wolf, G., 2006. Cell proliferation is influenced by bulbectomy and normalized by imipramine treatment in a region-specific manner. Neuropsychopharmacol.: Off. Publ. Am. Coll. Neuropsychopharmacol. 31, 1165–1176.
Kelly, J.P., Wrynn, A.S., Leonard, B.E., 1997. The olfactory bulbectomized rat as a model of depression: an update. Pharmacol. Ther. 74, 299–316.
Kettenmann, H., Hanisch, U.K., Noda, M., Verkhratsky, A., 2011. Physiology of microglia. Physiol. Rev. 91, 461–553.
Kilkenny, C., Browne, W.J., Cuthill, I.C., Emerson, M., Altman, D.G., 2010. Improving bioscience research reporting: the ARRIVE guidelines for reporting animal research. PLoS Biol. 8, e1000412.
Kolber, B.J., Montana, M.C., Carrasquillo, Y., Xu, J., Heinemann, S.F., Muglia, L.J. & Gereau, R.Wt (2010) Activation of metabotropic glutamate receptor 5 in the amygdala modulates pain-like behavior. The Journal of neuroscience: the official journal of the Society for Neuroscience, 30, 8203–8213.
LeDoux, J.E., Cicchetti, P., Xagoraris, A. & Romanski, L.M. (1990) The lateral amygdaloid nucleus: sensory interface of the amygdala in fear conditioning. The Journal of neuroscience: the official journal of the Society for Neuroscience, 10, 1062–1069.
Lenz, K.M., Nugent, B.M., Haliyur, R. & McCarthy, M.M. (2013) Microglia are essential to masculinization of brain and behavior. The Journal of neuroscience: the official journal of the Society for Neuroscience, 33, 2761–2772.
Lu, J.S., Yang, L., Chen, J., Xiong, F.F., Cai, P., Wang, X.Y., Xiong, B.J., Chen, Z.H., Chen, L., Yang, J., Yu, C.X., 2022. Basolateral amygdala astrocytes modulate diabetic neuropathic pain and may be a potential therapeutic target for koumine. Br. J. Pharmacol.
Machado, D.G., Lara, M.V.S., Dobler, P.B., Almeida, R.F., Porciuncula, L.O., 2020. Caffeine prevents neurodegeneration and behavioral alterations in a mice model of agitated depression. Prog. Neuro-Psychopharmacol. Biol. Psychiatry 98, 109776.
Martuscello, R.T., Spengler, R.N., Bonoiu, A.C., Davidson, B.A., Helinski, J., Ding, H., Mahajan, S., Kumar, R., Bergey, E.J., Knight, P.R., Prasad, P.N., Ignatowski, T.A., 2012. Increasing TNF levels solely in the rat hippocampus produces persistent pain-like symptoms. Pain 153, 1871–1882.
Miller, A.H., Raison, C.L., 2016. The role of inflammation in depression: from evolutionary imperative to modern treatment target. Nat. Rev. Immunol. 16, 22–34.
Monfil, T., Vazquez Roque, R.A., Camacho-Abrego, I., Tendilla-Beltran, H., Iannitti, T., Meneses-Morales, I., Aguilar-Alonso, P., Flores, G. & Morales-Medina, J.C. (2018) Hyper-response to Novelty Increases c-Fos Expression in the Hippocampus and Prefrontal Cortex in a Rat Model of Schizophrenia. Neurochemical research, 43, 441–448.
Morales-Medina, J.C., Dumont, Y., Benoit, C.E., Bastianetto, S., Flores, G.., Fournier, A. & Quirion, R.. (2012a) Role of neuropeptide Y Y(1) and Y(2) receptors on behavioral despair in a rat model of depression with co-morbid anxiety. Neuropharmacology, 62, 200–208.
Morales-Medina, J.C., Dumont, Y., Bonaventure, P., Quirion, R., 2012b. Chronic administration of the Y2 receptor antagonist, JNJ-31020028, induced anti-depressant like-behaviors in olfactory bulbectomized rat. Neuropeptides 46, 329–334.
Morales-Medina, J.C., Iannitti, T., Freeman, A., Caldwell, H.K., 2017. The olfactory bulbectomized rat as a model of depression: The hippocampal pathway. Behav. brain Res. 317, 562–575.
Morales-Medina, J.C., Juarez, I., Iannitti, T., Flores, G., 2013a. Olfactory bulbectomy induces neuronal rearrangement in the entorhinal cortex in the rat. J. Chem. Neuroanat. 52, 80–86.
Morales-Medina, J.C., Juarez, I., Venancio-Garcia, E., Cabrera, S.N., Menard, C., Yu, W., Flores, G., Mechawar, N., Quirion, R., 2013b. Impaired structural hippocampal plasticity is associated with emotional and memory deficits in the olfactory bulbectomized rat. Neuroscience 236, 233–243.
Morales-Medina, J.C., Mejorada, A., Romero-Curiel, A., Flores, G., 2007. Alterations in dendritic morphology of hippocampal neurons in adult rats after neonatal administration of N-omega-nitro-L-arginine. Synapse 61, 785–789.
Morales-Medina, J.C., Rastogi, A., Mintz, E., Caldwell, H.K., 2020. Increased immediate early gene activation in the basolateral amygdala following persistent peripheral inflammation. Neuroreport 31, 724–729.
Moriarty, O., Roche, M., McGuire, B.E., Finn, D.P., 2012. Validation of an air-puff passive-avoidance paradigm for assessment of aversive learning and memory in rat models of chronic pain. J. Neurosci. Methods 204, 1–8.
Munshi, S., Loh, M.K., Ferrara, N., DeJoseph, M.R., Ritger, A., Padival, M., Record, M.J., Urban, J.H., Rosenkranz, J.A., 2020. Repeated stress induces a pro-inflammatory state, increases amygdala neuronal and microglial activation, and causes anxiety in adult male rats. Brain, Behav., Immun. 84, 180–199.
Naskar, S., Chattarji, S., 2019. Stress Elicits Contrasting Effects on the Structure and Number of Astrocytes in the Amygdala versus Hippocampus. eNeuro **6**.
Oka, T., Oka, K., Hosoi, M., Hori, T., 1995. Intracerebroventricular injection of interleukin-6 induces thermal hyperalgesia in rats. Brain Res. 692, 123–128.
Ongur, D., Drevets, W.C., Price, J.L., 1998. Glial reduction in the subgenual prefrontal cortex in mood disorders. Proc. Natl. Acad. Sci. USA 95, 13290–13295.
Paxinos, G., Watson, C., 1997. The Rat Brainin Stereotaxic Coordinates, **Third edition**.,. Academic Press,, *San Diego*.

Phelps, E.A., LeDoux, J.E., 2005. Contributions of the amygdala to emotion processing: from animal models to human behavior. Neuron 48, 175–187.
Poyhonen, S., Er, S., Domanskyi, A., Airavaara, M., 2019. Effects of Neurotrophic Factors in Glial Cells in the Central Nervous System: Expression and Properties in Neurodegeneration and Injury. Front. Physiol. 10, 486.
Rajkumar, R., Dawe, G.S., 2018. OBscure but not OBsolete: Perturbations of the frontal cortex in common between rodent olfactory bulbectomy model and major depression. J. Chem. Neuroanat. 91, 63–100.
Sanacora, G., Banasr, M., 2013. From pathophysiology to novel antidepressant drugs: glial contributions to the pathology and treatment of mood disorders. Biol. Psychiatry 73, 1172–1179.
Schafer, D.P., Lehrman, E.K., Stevens, B., 2013. The "quad-partite" synapse: microglia-synapse interactions in the developing and mature CNS. Glia 61, 24–36.
Sholl, D.A., 1953. Dendritic organization in the neurons of the visual and motor cortices of the cat. J. Anat. 87, 387–406.
Si, X., Miguel-Hidalgo, J.J., O'Dwyer, G., Stockmeier, C.A., Rajkowska, G., 2004. Age-dependent reductions in the level of glial fibrillary acidic protein in the prefrontal cortex in major depression. Neuropsychopharmacol.: Off. Publ. Am. Coll. Neuropsychopharmacol. 29, 2088–2096.
Stockmeier, C.A., Mahajan, G.J., Konick, L.C., Overholser, J.C., Jurjus, G.J., Meltzer, H. Y., Uylings, H.B., Friedman, L., Rajkowska, G., 2004. Cellular changes in the postmortem hippocampus in major depression. Biol. Psychiatry 56, 640–650.
Takahashi, K., Nakagawasai, O., Nemoto, W., Kadota, S., Isono, J., Odaira, T., Sakuma, W., Arai, Y., Tadano, T., Tan-No, K., 2018. Memantine ameliorates depressive-like behaviors by regulating hippocampal cell proliferation and neuroprotection in olfactory bulbectomized mice. Neuropharmacology 137, 141–155.
Taylor, B.K., Abhyankar, S.S., Vo, N.T., Kriedt, C.L., Churi, S.B., Urban, J.H., 2007. Neuropeptide Y acts at Y1 receptors in the rostral ventral medulla to inhibit neuropathic pain. Pain 131, 83–95.
Torres-Platas, S.G., Hercher, C., Davoli, M.A., Maussion, G., Labonte, B., Turecki, G., Mechawar, N., 2011. Astrocytic hypertrophy in anterior cingulate white matter of depressed suicides. Neuropsychopharmacol.: Off. Publ. Am. Coll. Neuropsychopharmacol. 36, 2650–2658.
Torres-Platas, S.G., Nagy, C., Wakid, M., Turecki, G., Mechawar, N., 2016. Glial fibrillary acidic protein is differentially expressed across cortical and subcortical regions in healthy brains and downregulated in the thalamus and caudate nucleus of depressed suicides. Mol. Psychiatry 21, 509–515.
Tynan, R.J., Beynon, S.B., Hinwood, M., Johnson, S.J., Nilsson, M., Woods, J.J., Walker, F.R., 2013. Chronic stress-induced disruption of the astrocyte network is driven by structural atrophy and not loss of astrocytes. Acta Neuropathol. 126, 75–91.
von Knorring, L., Perris, C., Eisemann, M., Eriksson, U., Perris, H., 1983. Pain as a symptom in depressive disorders. II. Relationship to personality traits as assessed by means of KSP. Pain 17, 377–384.
Wang, W., Qi, W.J., Xu, Y., Wang, J.Y., Luo, F., 2010. The differential effects of depression on evoked and spontaneous pain behaviors in olfactory bulbectomized rats. Neurosci. Lett. 472, 143–147.
W.H.O., 2017, Depression and other common mental disorders: global health stimates. Geneva.
Wohleb, E.S., Franklin, T., Iwata, M., Duman, R.S., 2016. Integrating neuroimmune systems in the neurobiology of depression. Nat. Rev. Neurosci. 17, 497–511.
Worthen, R.J., Garzon Zighelboim, S.S., Torres Jaramillo, C.S., Beurel, E., 2020. Anti-inflammatory IL-10 administration rescues depression-associated learning and memory deficits in mice. J. Neuroinflamm. 17, 246.
Xiao, K., Luo, Y., Liang, X., Tang, J., Wang, J., Xiao, Q., Qi, Y., Li, Y., Zhu, P., Yang, H., Xie, Y., Wu, H., Tang, Y., 2021. Beneficial effects of running exercise on hippocampal microglia and neuroinflammation in chronic unpredictable stress-induced depression model rats. Transl. Psychiatry 11, 461.
Yanguas-Casas, N., Crespo-Castrillo, A., Arevalo, M.A., Garcia-Segura, L.M., 2020. Aging and sex: Impact on microglia phagocytosis. Aging Cell 19, e13182.
Yoshimura, S., Ueda, K., Suzuki, S., Onoda, K., Okamoto, Y., Yamawaki, S., 2009. Self-referential processing of negative stimuli within the ventral anterior cingulate gyrus and right amygdala. Brain Cogn. 69, 218–225.
Yuan, T., Manohar, K., Latorre, R., Orock, A., Greenwood-Van Meerveld, B., 2020. Inhibition of microglial activation in the amygdala reverses stress-induced abdominal pain in the male rat. Cell Mol. Gastroenterol. Hepatol. 10, 527–543.
Zhang, L., Verwer, R.W.H., Zhao, J., Huitinga, I., Lucassen, P.J., Swaab, D.F., 2021. Changes in glial gene expression in the prefrontal cortex in relation to major depressive disorder, suicide and psychotic features. J. Affect. Disord. 295, 893–903.
Zhao, Y.F., Verkhratsky, A., Tang, Y., Illes, P., 2022. Astrocytes and major depression: The purinergic avenue. Neuropharmacology 220, 109252.